Hindawi
Advances in High Energy Physics
Volume 2021, Article ID 8822524, 19 pages
https://doi.org/10.1155/2021/8822524

Research Article

Event Shape and Multiplicity Dependence of Freeze-Out Scenario and System Thermodynamics in Proton+Proton Collisions at $\sqrt{s} = 13$ TeV Using PYTHIA8

Sushanta Tripathy,[1] **Ashish Bisht**,[1] **Raghunath Sahoo**,[1] **Arvind Khuntia**,[2] **and Malavika Panikkassery Salvan**[3]

[1]*Department of Physics, Indian Institute of Technology Indore, Simrol, Indore 453552, India*
[2]*Institute of Nuclear Physics, Polish Academy of Science (PAS), IFJ PAN, Krakow, Poland*
[3]*National Institute of Technology Tiruchirappalli, Tiruchirappalli, Tamil Nadu, India*

Correspondence should be addressed to Raghunath Sahoo; raghunath.sahoo@cern.ch

Received 24 September 2020; Revised 28 December 2020; Accepted 18 January 2021; Published 23 February 2021

Academic Editor: Mariana Frank

Recent observations of QGP-like conditions in high-multiplicity pp collisions from ALICE experiment at the LHC warrant an introspection whether to use pp collisions as a baseline measurement to characterize heavy-ion collisions for the possible formation of a Quark-Gluon Plasma. A double differential study of the particle spectra and thermodynamics of the produced system as a function of charged-particle multiplicity and transverse spherocity in pp collisions would shed light on the underlying event dynamics. Transverse spherocity, one of the event shape observables, allows to separate the events in terms of jetty and isotropic events. We analyse the identified particle transverse momentum (p_T) spectra as a function of charged-particle multiplicity and transverse spherocity using Tsallis nonextensive statistics and Boltzmann-Gibbs Blast-Wave (BGBW) model in pp collisions at $\sqrt{s} = 13$ TeV using PYTHIA8 event generator. The extracted parameters such as temperature (T), radial flow (β), and nonextensive parameter (q) are shown as a function of charged-particle multiplicity for different spherocity classes. We observe that the isotropic events approach thermal equilibrium while the jetty ones remain far from equilibrium. We argue that, while studying the QGP-like conditions in small systems, one should separate the isotropic events from the spherocity-integrated events, as the production dynamics are different.

1. Introduction

Although it was envisaged long back that central heavy-ion collisions at ultrarelativistic energies could produce a deconfined state of partons called Quark-Gluon Plasma (QGP) [1, 2], the unprecedented collision energies available at the Large Hadron Collider (LHC) at CERN, Switzerland, has brought up new challenges in characterizing the proton+proton (pp) collisions to understand a possible formation of QGP droplets in these hadronic collisions. There are various signatures of QGP, which are already observed in pp collisions at the LHC. These include strangeness enhancement [3], hardening of p_T-spectra [4, 5], and the thermal effective temperature being comparable to that observed in heavy-ion collisions [3], degree of collectivity [6], etc. In view of these observations in pp collisions, it has become more challenging to understand the system formed in pp collisions, although pp has been considered as a baseline measurement to understand nuclear effects like R_{AA} and suppression of J/ψ. The new measurements at the LHC keeping in mind that the final state multiplicity drives the particle production (excellent scaling observed) necessiate a closer look into the underlying physics mechanisms of particle production in pp collisions. The phenomena like color reconnection, multipartonic interactions, rope hadronization, and string fragmentation have done a wonderful job

Table 1: V0 multiplicity classes and the corresponding charged particle multiplicities.

V0M class	I	II	III	IV	V	VI	VII	VIII	IX	X
N_{ch}	50-140	42-49	36-41	31-35	27-30	23-26	19-22	15-18	10-14	0-9

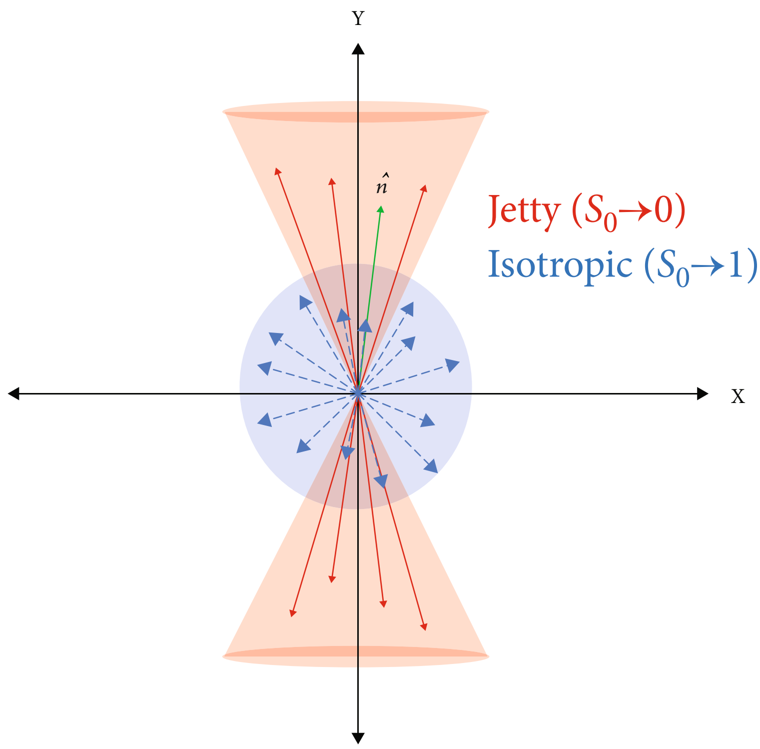

Figure 1: (Color online) Figure showing jetty and isotropic events in the transverse plane.

in explaining various new heavy-ion-like observations in pp collisions.

Event shape engineering has given a new direction to underlying events in pp collisions to have a differential study taking various observables. The transverse spherocity successfully separates jetty events from isotropic ones in pp collisions. As is clearly understandable, the particle production mechanism in jetty events is different from isotropic ones. When the former one involves high-p_T phenomena, the latter is soft-physics dominated. In view of this, recently, we have carried out a double differential study of particle ratios in pp collisions at the LHC energies, taking transverse spherocity, transverse momentum, and multiplicity [7]. A natural question which pops up is whether the thermodynamics of jetty events are different from the isotropic ones. To quantify this, in the present study, we have taken pQCD-inspired PYTHIA8 event generator which includes multiparton interactions (MPI) along with color reconnection (CR), to study the event shape and multiplicity dependence of freeze-out scenario and system thermodynamics in pp collisions at $\sqrt{s} = 13$ TeV. It has been reported that the MPI scenario is crucial to explain the underlying events, multiplicity distributions, and flow-like patterns in terms of color reconnection [8]. Thus, it is a preferable tune to study the possible thermodynamics in small systems, as experimental data are not available yet. It should be worth noting that PYTHIA8 does not have inbuilt thermalization. However, as reported in Ref. [8], the color reconnection (CR) mechanism along with the multipartonic interactions (MPI) in PYTHIA8 produces the properties which arise from the thermalization of a system such as radial flow and mass dependent rise of mean transverse momentum. In the PYTHIA model, a single string connecting two partons follows the movement of the partonic endpoints, and this movement gives a common boost to the string fragments (final state hadrons). With CR along with MPI, two partons from independent hard scatterings can reconnect and they increase the transverse boost. This microscopic treatment of final state particle production is quite successful in explaining the similar features which arise from a macroscopic picture via hydrodynamical description of high-energy collisions. Thus, it is apparent to say that the PYTHIA8 model with MPI and CR has a plausible ability to produce the features of thermalization. The current results, which use PYTHIA8 with MPI and CR to obtain event shape and multiplicity dependence of freeze-out scenario and

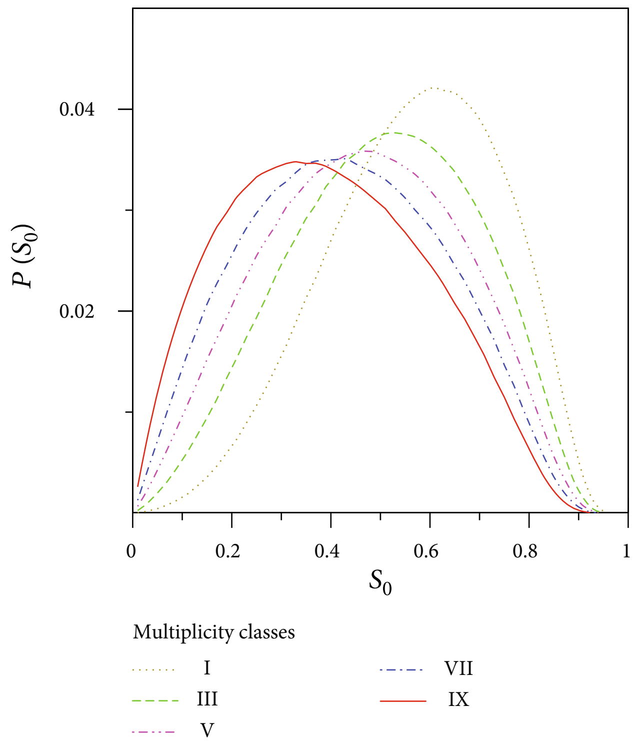

Figure 2: (Color online) Spherocity distribution for different multiplicity classes in pp collisions at $\sqrt{s} = 13$ TeV using PYTHIA8. Different colors and line styles are for different multiplicity classes.

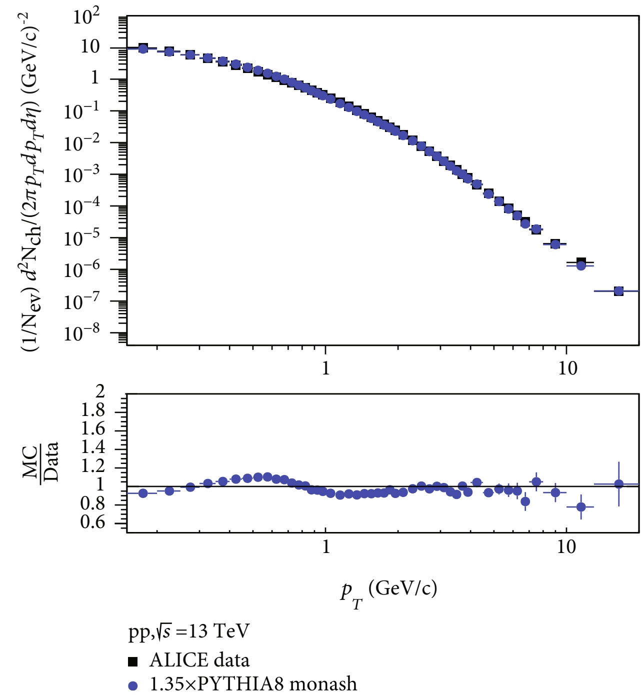

Figure 3: (Color online) Upper panel: comparison of charged particle p_T spectra in pp collisions at $\sqrt{s} = 13$ TeV between ALICE data [19] and PYTHIA8 simulation, which is used for this analysis. Lower panel: the ratio between scaled simulated data and experimental data.

system thermodynamics, will help to compare with the upcoming experimental data. Such a study has also been done for heavy flavor particles like J/ψ in Ref. [9]. This paper is intended solely for presenting a noble and unique study, which would give an outlook on similarities/differences between jetty and isotropic events in LHC pp events and their multiplicity dependence. This will help in making a proper bridge in understanding the particle production from hadronic to heavy-ion collisions.

Furthermore, the spacetime evolution of hadronic and heavy-ion collisions at the LHC energies could be thought of following a cosmological expansion of the produced fireball. In this scenario, as the fireball expands and cools down, it leaves a temperature profile with time. Different identified particles decouple from the fireball giving the signature of a mass-dependent particle freeze-out—higher mass particles decoupling from the system earlier in time. In this work, we have considered such a scenario and have performed a differential study taking final state event multiplicity and event topology.

The paper is organized as follows. After the introduction and identification of the problem under consideration, we discuss the methodology of event generation and data analysis in Section 2. In Section 3, we discuss the identified p_T-spectra in pp collisions to extract the thermodynamic parameters. Finally, we summarize the work in Section 4 with important findings, which could be tested when experimental data become available.

2. Event Generation and Analysis Methodology

PYTHIA, one of the popular and most useful event generators in the LHC era, is used to simulate ultrarelativistic collision events among the elementary particles like $e^{\pm}$, p, and $\bar{p}$. It is incorporated with many known physics mechanisms like hard and soft interactions, parton distributions, initial- and final-state parton showers, multipartonic interactions, string fragmentation, color reconnection, and resonance decays [10].

In our present study, we have used PYTHIA 8.235 to generate pp collisions at $\sqrt{s} = 13$ TeV with Monash 2013 Tune (Tune:14) [11]. PYTHIA 8.235 is an advanced version of PYTHIA 6 which includes the multipartonic interaction (MPI) scenario as one of the key improvements. The detailed physics processes in PYTHIA 8.235 can be found in Ref. [12]. We have implemented the inelastic, nondiffractive component of the total cross-section for all soft QCD processes with the switch SoftQCD: all = on. This analysis is carried out with around 250 million minimum bias events at $\sqrt{s} = 13$ TeV, and we have chosen MPI-based scheme of default color reconnection mode (ColorReconnection:mode(0)). Here, the minimum bias events are those events where no selection on charged-particle multiplicity and/or spherocity is applied. For the generated events, we let all the resonances to decay except the ones used in our study with the switch HadronLevel:Decay = on. Throughout the analysis, the event selection criteria are such that only those events were chosen

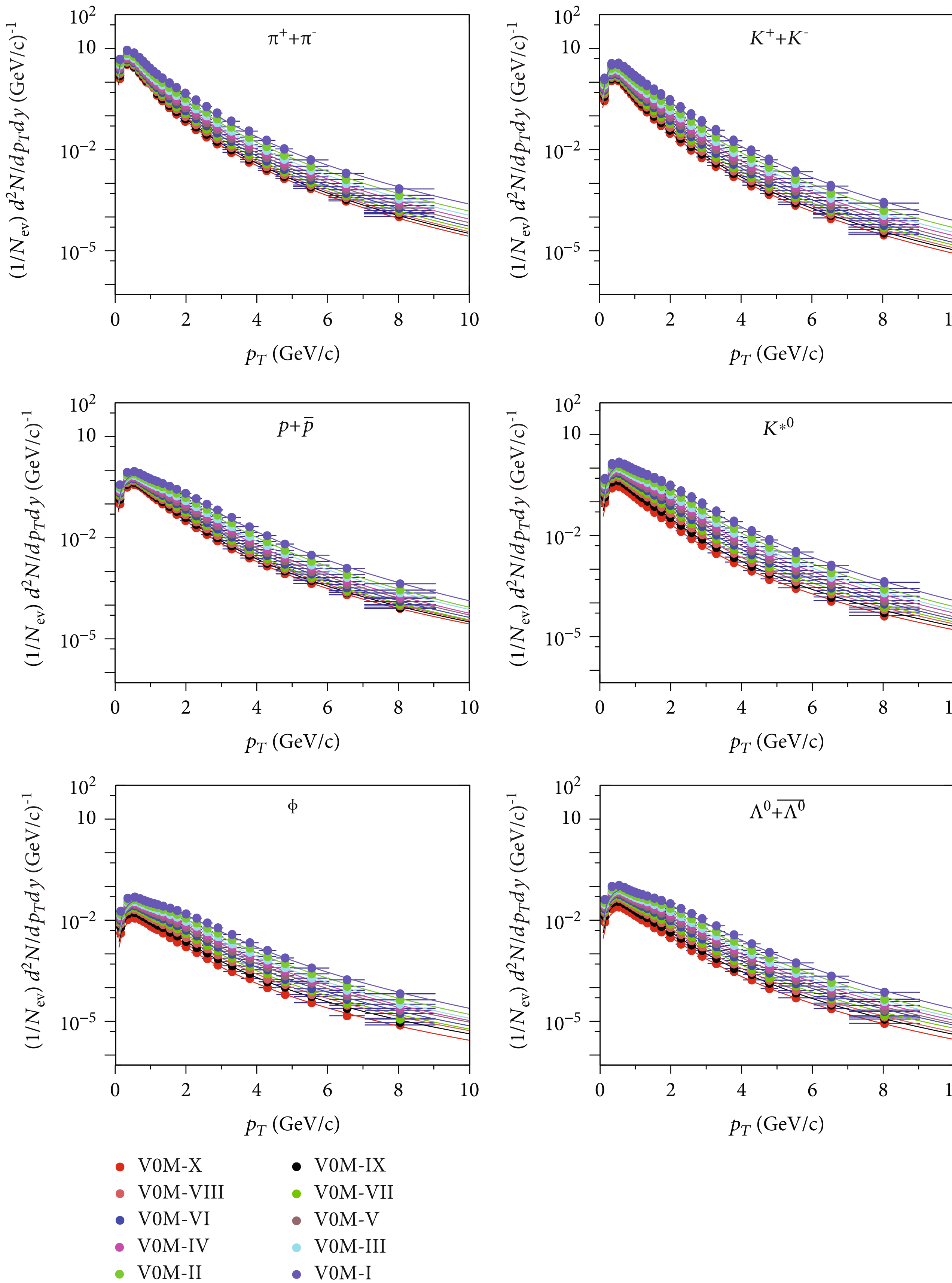

Figure 4: (Color online) Fitting of generated p_T-spectra of identified hadrons from PYTHIA8 using Tsallis distribution for spherocity integrated events in various multiplicity classes as shown in Table 1.

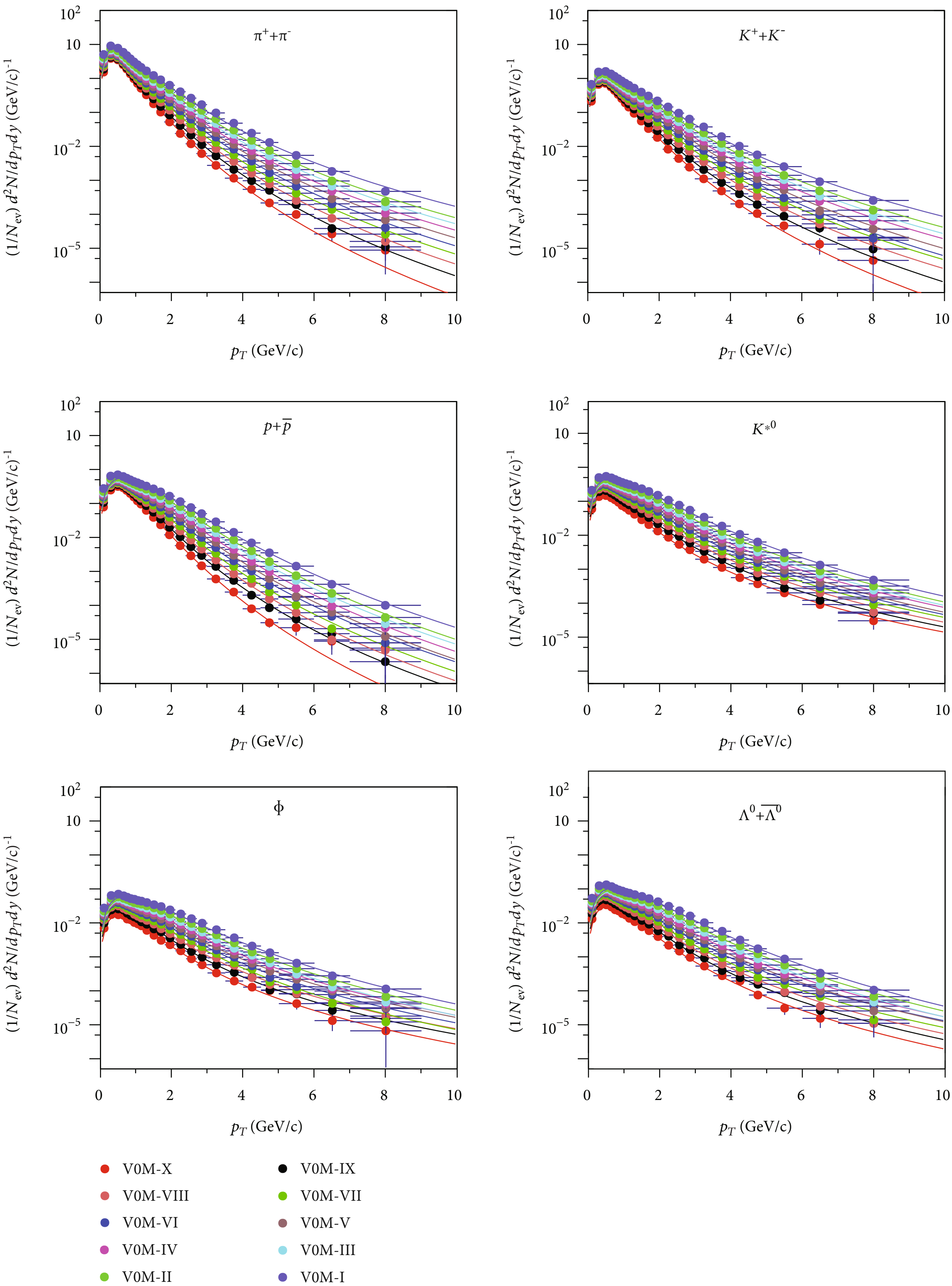

FIGURE 5: (Color online) Fitting of generated p_T-spectra of identified hadrons from PYTHIA8 using Tsallis distribution for isotropic events in various multiplicity classes as shown in Table 1.

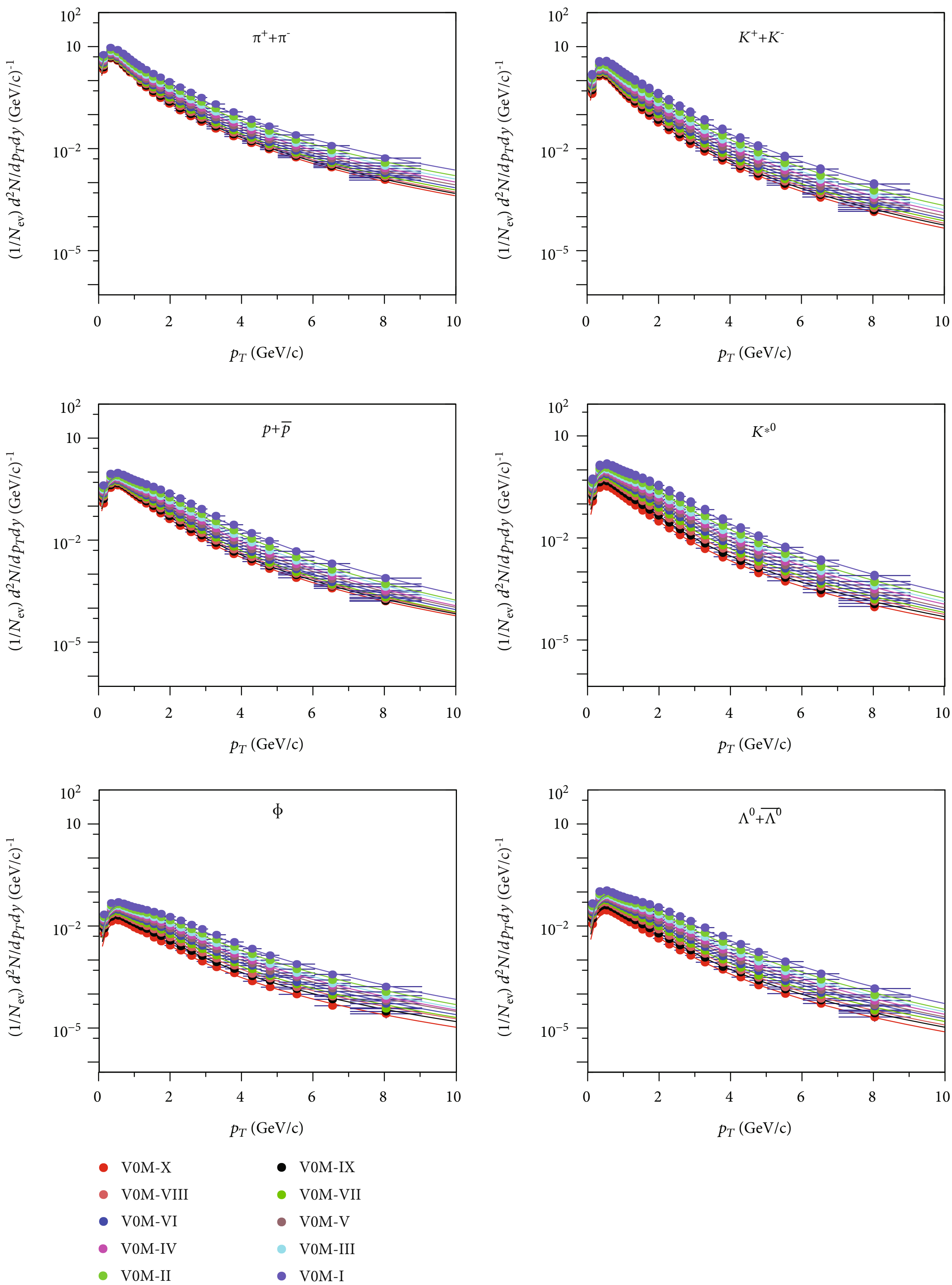

Figure 6: (Color online) Fitting of generated p_T-spectra of identified hadrons from PYTHIA8 using Tsallis distribution for jetty events in various multiplicity classes as shown in Table 1.

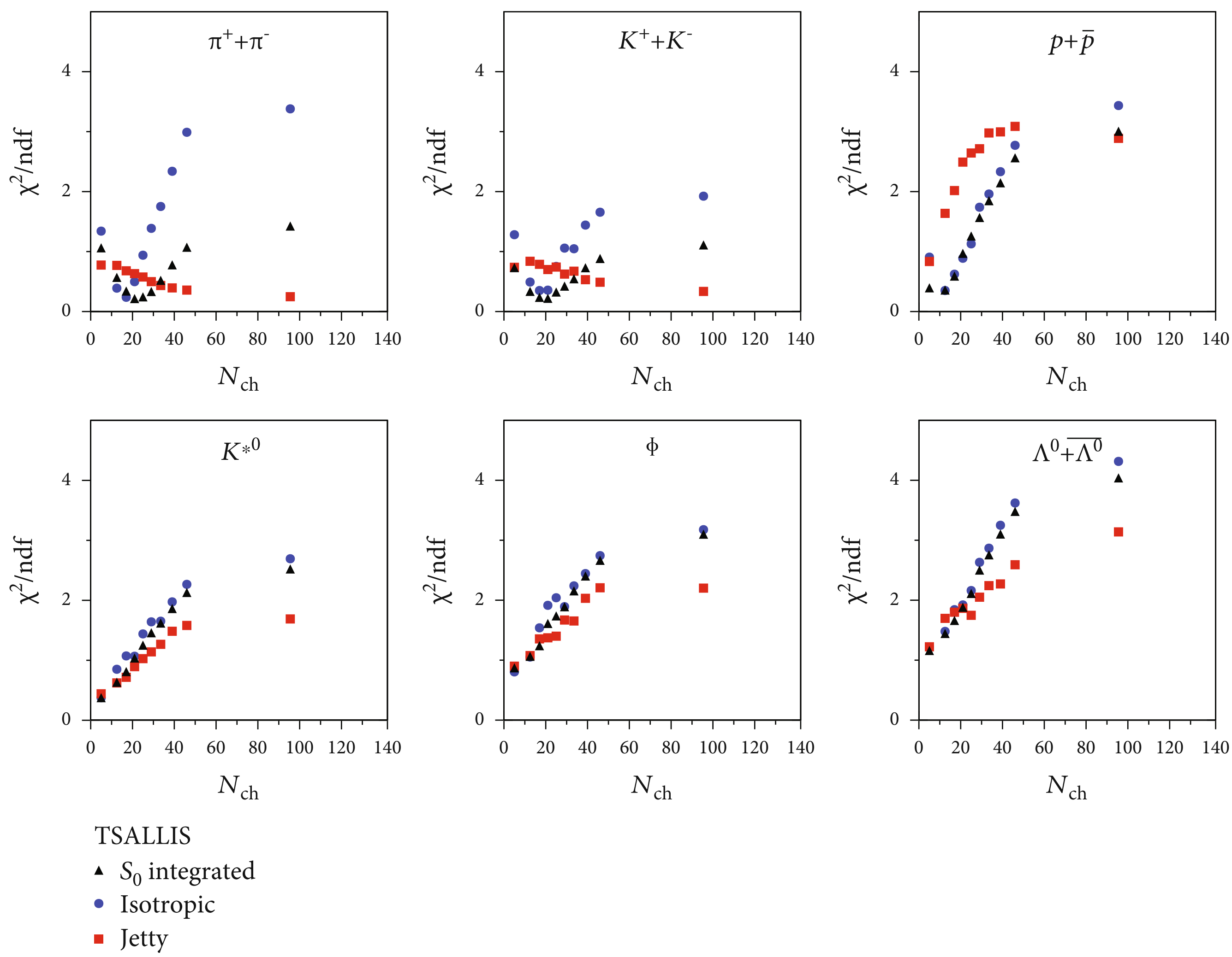

Figure 7: (Color online) χ^2/NDF for the fitting of generated p_T-spectra of identified hadrons using Tsallis distribution in different spherocity and multiplicity classes.

which have at least 5 charged particles. To match with experimental conditions, charged particle multiplicities (N_{ch}) have been chosen in the acceptance of V0 detector in ALICE at the LHC with pseudorapidity coverage of V0A ($2.8 < \eta < 5.1$) and V0C ($-3.7 < \eta < -1.7$) [13]. The generated events are categorized in ten V0 multiplicity (V0M) bins, each with 10% of the total number of events. The number of charged particle multiplicities in an event in different V0 multiplicity classes is listed in Table 1.

For an event, transverse spherocity is defined for a unit vector $\hat{n}(n_T, 0)$ which minimizes the ratio [14–16]:

$$S_0 = \frac{\pi^2}{4}\left(\frac{\Sigma_i\left|\vec{p}_{T_i} \times \hat{n}\right|}{\Sigma_i p_{T_i}}\right)^2. \quad (1)$$

By restricting it to the transverse plane, transverse spherocity becomes infrared and collinear safe [17], and by construction, the extreme limits of transverse spherocity are related to specific configurations of events in the transverse plane. The value of transverse spherocity ranges from 0 to 1. Transverse spherocity becoming 0 means that the events are pencil-like (back-to-back structure) while 1 would mean the events are isotropic as shown in Figure 1. The pencil-like events are usually the hard events, while the isotropic events are the result of soft processes. Here onwards, for the sake of simplicity, the transverse spherocity is referred to as spherocity. To disentangle the jetty and isotropic events from the average-shaped events, we have applied spherocity cuts on our generated events. In this analysis, the spherocity distributions are selected in the pseudorapidity range of $|\eta| < 0.8$ with a minimum constraint of 5 charged particles with p_T>0.15 GeV/c. The jetty events are those having $0 \le S_0 < 0.29$ with lowest 20 percent (≃50 M events), and the isotropic events are those having $0.64 < S_0 \le 1$ with highest 20 percent (≃50 M events) of the total events [18].

To assure the quality of the generated events, we show in Figure 2, the correlation between the spherocity with

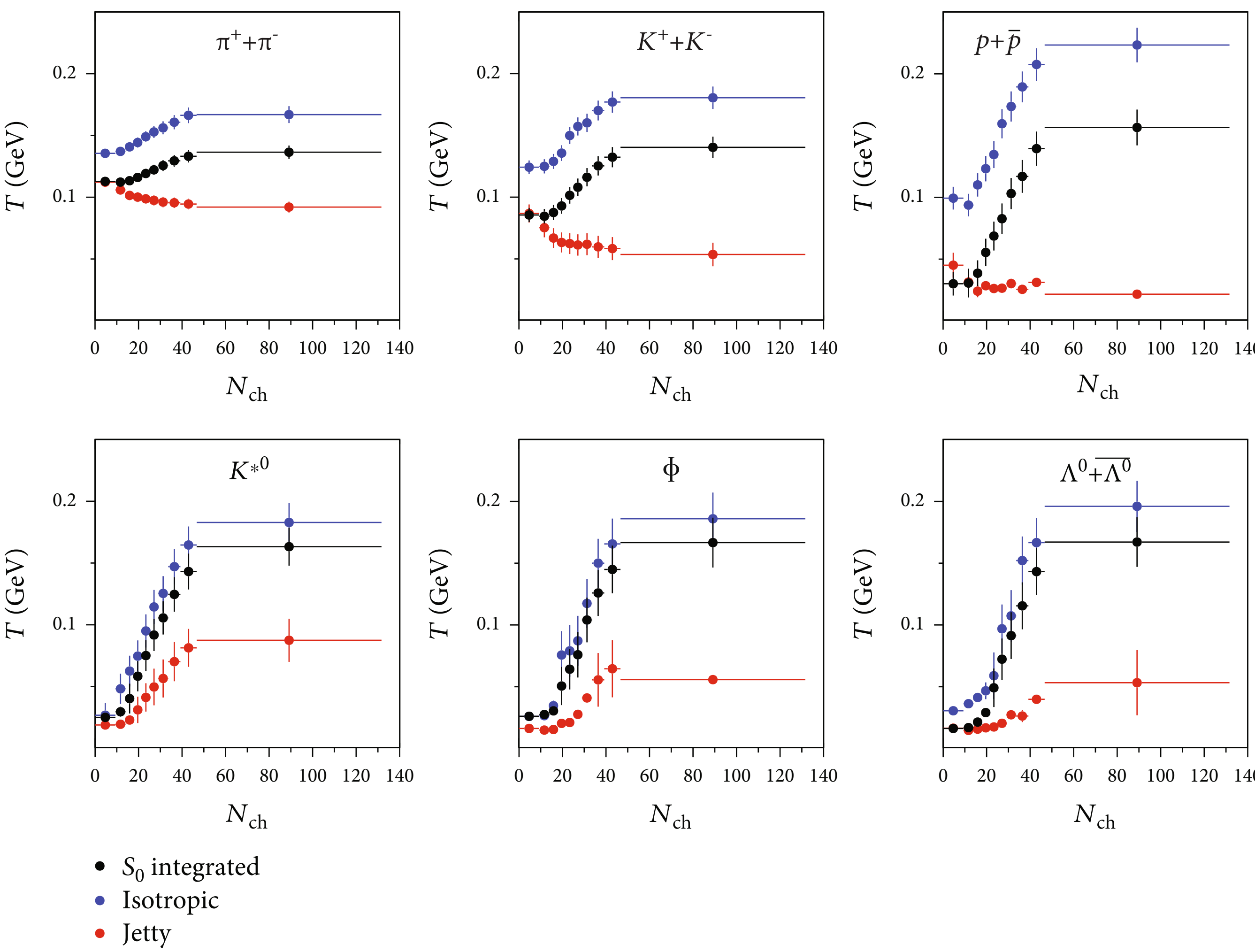

FIGURE 8: (Color online) Multiplicity dependence of T in different spherocity classes from the fitting of Tsallis distribution using Eq. (4).

charged-particle multiplicity. As expected, the high multiplicity pp collisions are dominated by isotropic events, while the low multiplicity events are dominated by the jetty ones. From our earlier event shape analysis [7], it is evident that spherocity along with the charged particle multiplicity (which is correlated with nMPI) should be preferred for a better selectivity of events.

3. Transverse Momentum Spectra of Identified Particles

To check the compatibility of PYTHIA8 simulated data with the experimental data, we have compared the charged particle p_T spectra for pp collisions at $\sqrt{s} = 13$ TeV from ALICE data [19]. The comparison is shown in Figure 3. The lower panel shows the ratio of the predictions from PYTHIA8 to experimental data. In order to see the agreement of spectral shapes, we have used an arbitrary scaling factor (1.35) to scale the simulated data. The used scaling factor is to check the matching of the spectral shape, and it bears no physical significance. We found that the scaled simulated data agree with the spectral shape from experimental data within (10-20)% at low-p_T and consistent to unity for intermediate and high-p_T.

For the first time, we combine spherocity with event multiplicity and study the freeze-out scenario and thermodynamics of the system formed in pp collisions at $\sqrt{s} = 13$ TeV. We use experimentally motivated thermodynamically consistent Tsallis nonextensive distribution function [20] for analysing the complete range of the p_T-spectra, whereas to extract the kinetic freeze-out temperature and the possible collective radial flow we use the Boltzmann-Gibbs Blast-Wave model [21, 22] taking $p_T \leq 2$ GeV/c. We begin with the fitting and analysis procedure with a short description on Tsallis nonextensive statistics and Boltzmann-Gibbs Blast-Wave model. Here onwards, $(\pi^+ + \pi^-)$, $(K^+ + K^-)$, $(p + \bar{p})$, $(K^{*0} + \overline{K^{*0}})$, and $(\Lambda^0 + \overline{\Lambda^0})$ are denoted as pion (π), kaon (K), proton (p), K^{*0}, and Λ, respectively.

3.1. Experimentally Motivated Tsallis Nonextensive Statistics. The p_T-spectra of produced particles in high-energy

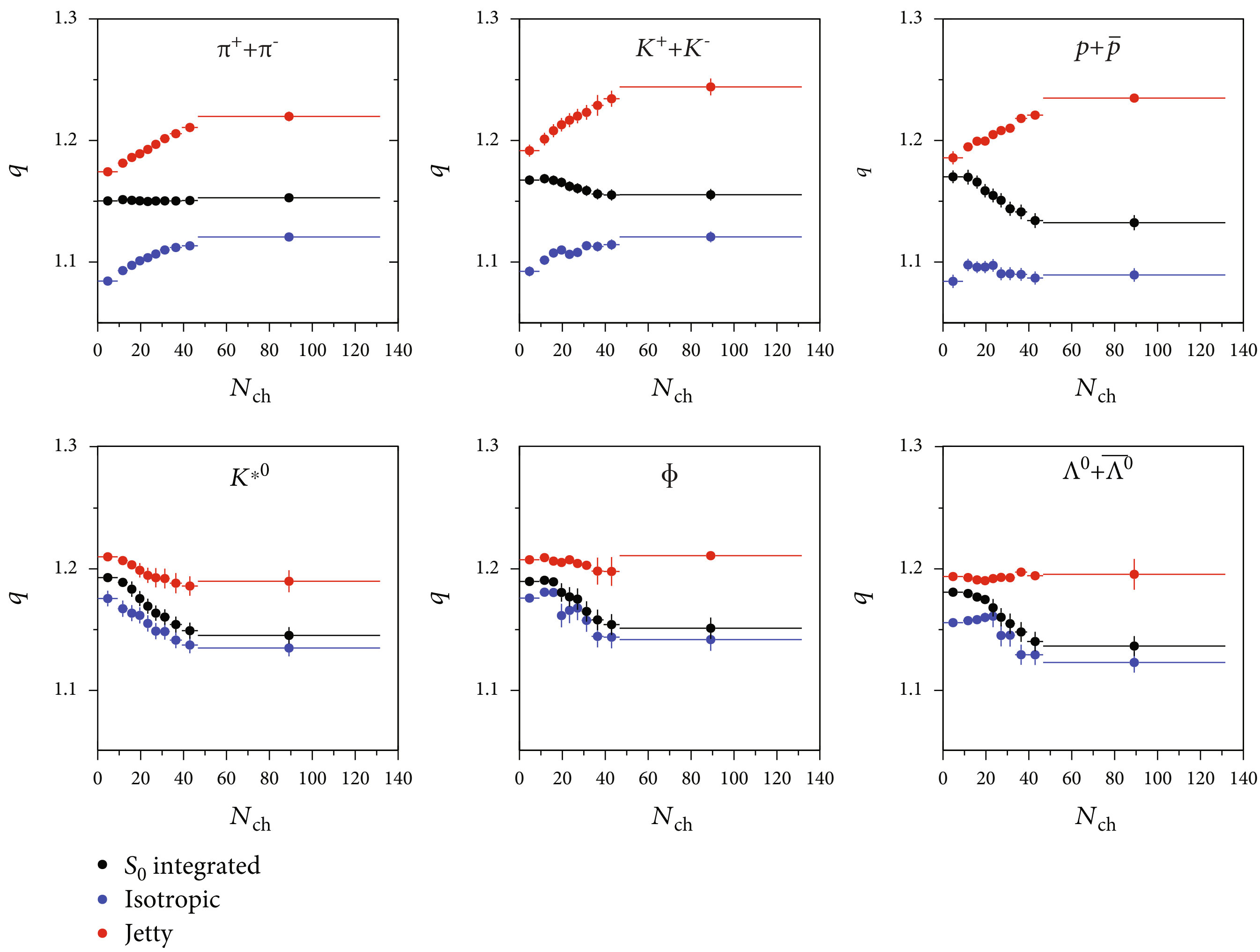

FIGURE 9: (Color online) Multiplicity dependence of q in different spherocity classes from the fitting of Tsallis distribution using Eq. (4).

collisions have been proposed to follow a thermalised Boltzmann type of distribution given as [23],

$$E\frac{d^3\sigma}{d^3p} \simeq C \exp\left(-\frac{p_T}{T_{kin}}\right). \quad (2)$$

Here, C is the normalisation constant, and T_{kin} is the kinetic freeze-out temperature. Due to possible QCD contributions at high-p_T, the identified particle spectra at RHIC and LHC do not follow the above distribution, while the low-p_T-region can be explained by incorporating the radial flow (β) into the Boltzmann-Gibbs distribution function, which is known as Boltzmann-Gibbs Blast-Wave (BGBW) model [22]. One can extract T_{kin} and radial flow (β) by fitting the identified particle transverse momentum spectra at low-p_T. The detailed description along with the fitting of the Boltzmann-Gibbs Blast-Wave model to the identified particle spectra is discussed in the next subsection.

To describe the complete p_T-spectra, one has to account for the power-law contribution at high-p_T [24–26], which empirically takes care of the possible QCD contributions. A combination of both low and high-p_T aspects has been proposed by Hagedorn, which describes the experimental data over a wide p_T-range [27]. The distribution proposed by Hagedorn is given by

$$E\frac{d^3\sigma}{d^3p} = C\left(1+\frac{p_T}{p_0}\right)^{-n} \longrightarrow \begin{cases} \exp\left(-\frac{np_T}{p_0}\right) & \text{for } p_T \longrightarrow 0, \\ \left(\frac{p_0}{p_T}\right)^n & \text{for } p_T \longrightarrow \infty. \end{cases} \quad (3)$$

Here, C, p_0, and n are fitting parameters. The above expression acts as an exponential and a power-law function for low and high-p_T, respectively. However, deviations are observed by experiments at RHIC [28, 29] and LHC [30–33] while describing the p_T-spectra of identified particles using a Boltzmann-Gibbs distribution function, even if the domain of temperature of the produced systems are high enough. On the other hand, Tsallis statistics with its nonextensivity features can be regarded as a generalization of Boltzmann-Gibbs statistics, and it gives a better description of systems, which have not yet reached equilibration. Its low-p_T exponential and high-p_T power-law behavior gives a complete spectral description of identified secondaries produced in pp collisions. In addition, a nonextensive entropic q-parameter shows the extent of nonequilibration of any particle in a thermal bath. There are few different versions of Tsallis distribution, which are being used by experimentalists and theoreticians. However, we use a thermodynamically consistent Tsallis nonextensive distribution function as shown in Ref. [20]. By saying thermodynamically consistent, we mean that the used distribution function satisfies all the standard thermodynamic relations for entropy, temperature, energy, pressure, and number density. The Tsallis distribution function at midrapidity is given by,

$$\frac{1}{p_T}\frac{d^2N}{dp_T dy}\bigg|_{y=0} = \frac{gVm_T}{(2\pi)^2}\left[1+(q-1)\frac{m_T}{T}\right]^{-q/(q-1)}, \qquad (4)$$

where g is the degeneracy factor, V is the system volume, $m_T = \sqrt{p_T^2+m^2}$ is the transverse mass, and q is the nonextensive parameter. In the limit of $q \longrightarrow 1$, Tsallis distribution (Eq. (4)) reduces to the standard Boltzmann-Gibbs distribution (Eq. (2)). It should be noted here that the use of the Tsallis nonextensive distribution function is purely motivated by its excellent description of experimental particle spectra. It has been widely used to explain the particle spectra in high-energy collisions [34–38] starting from elementary $e^+ + e^-$ and hadronic to heavy-ion collisions [28, 29, 39–52]. Recently, few comprehensive studies have been carried out using Tsallis distribution for pions and quarkonium spectra in pp collisions [53, 54]. In this subsection, we employ the Tsallis nonextensive distribution function as shown in Eq. (4) to describe the p_T-spectra. It should be noted here that the used Tsallis distribution function of Eq. (4) [55] has an extra power q, compared to the original distribution function proposed by Tsallis [56]. However, this form of the distribution function is thermodynamically consistent, which makes no major change in the observables as the values of q in hadronic collisions lie between, $1 \le q \le 1.22$ [57]. While Tsallis nonextensive statistics makes a connection between entropy and thermodynamics of a system, the dynamics of the system in terms of long-range correlations and fluctuations ($(q-1)$ being the strength of the fluctuation [58]) are encoded in the entropic parameter, q.

Figures 4–6 show the fitting of p_T-spectra of pions, kaons, protons, K^{*0}, ϕ, and Λ as a function of charged-particle multiplicity using Tsallis distribution function (Eq. (4)) for spherocity-integrated, isotropic, and jetty events, respectively. We observe that the Tsallis distribution fits the generated data till $p_T \simeq 10\,\mathrm{GeV/c}$. Figure 7 shows the quality of fitting in terms of the reduced-χ^2, χ^2/NDF as a function of multiplicity for different spherocity classes. The values of χ^2/NDF show that the quality of fitting is reasonably good for all the multiplicity and spherocity classes.

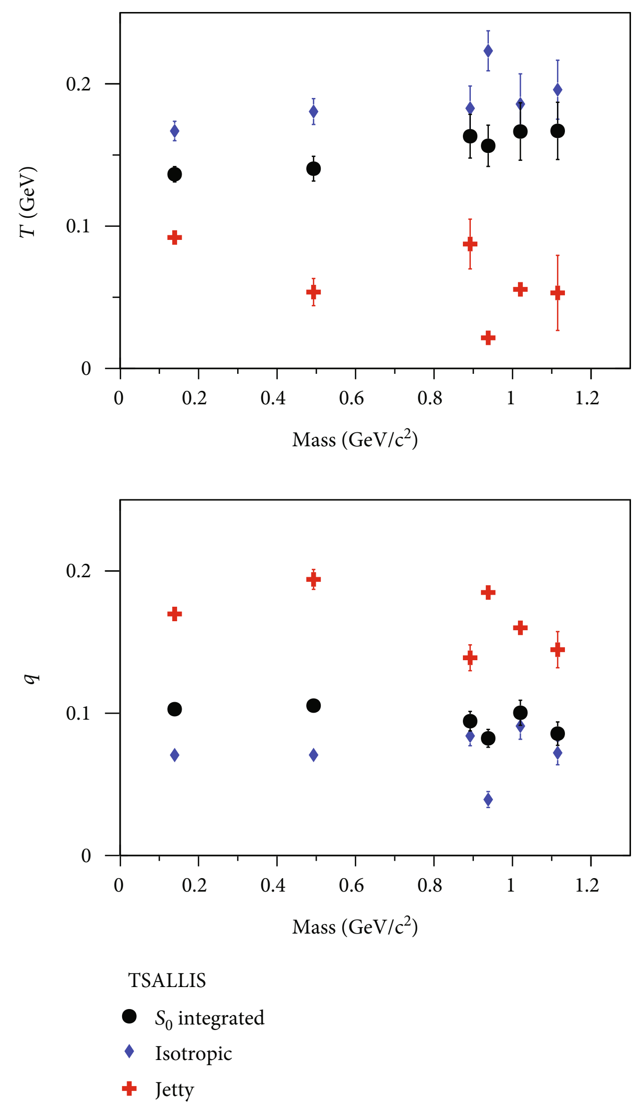

FIGURE 10: (Color online) Mass dependence of T and q in different spherocity classes for the highest multiplicity class.

Figures 8 and 9 show the extracted parameters from the fitting of Tsallis distribution using Eq. (4) as a function of charged-particle multiplicity for different spherocity classes. Figure 8 shows that the temperature parameter increases with charged-particle multiplicity for spherocity-integrated and isotropic events. However, the jetty events seem to show a reverse trend for pions, kaons, and protons. For K^{*0}, ϕ, and Λ, the temperature parameter shows an increase with multiplicity for jetty events. For all cases, the temperature for jetty events is lower compared to the other spherocity classes. We also observe that the temperature for lighter particles does not change significantly with multiplicity, while with the increase in mass, the temperature increases steeply as a function of multiplicity. Figure 9 shows that

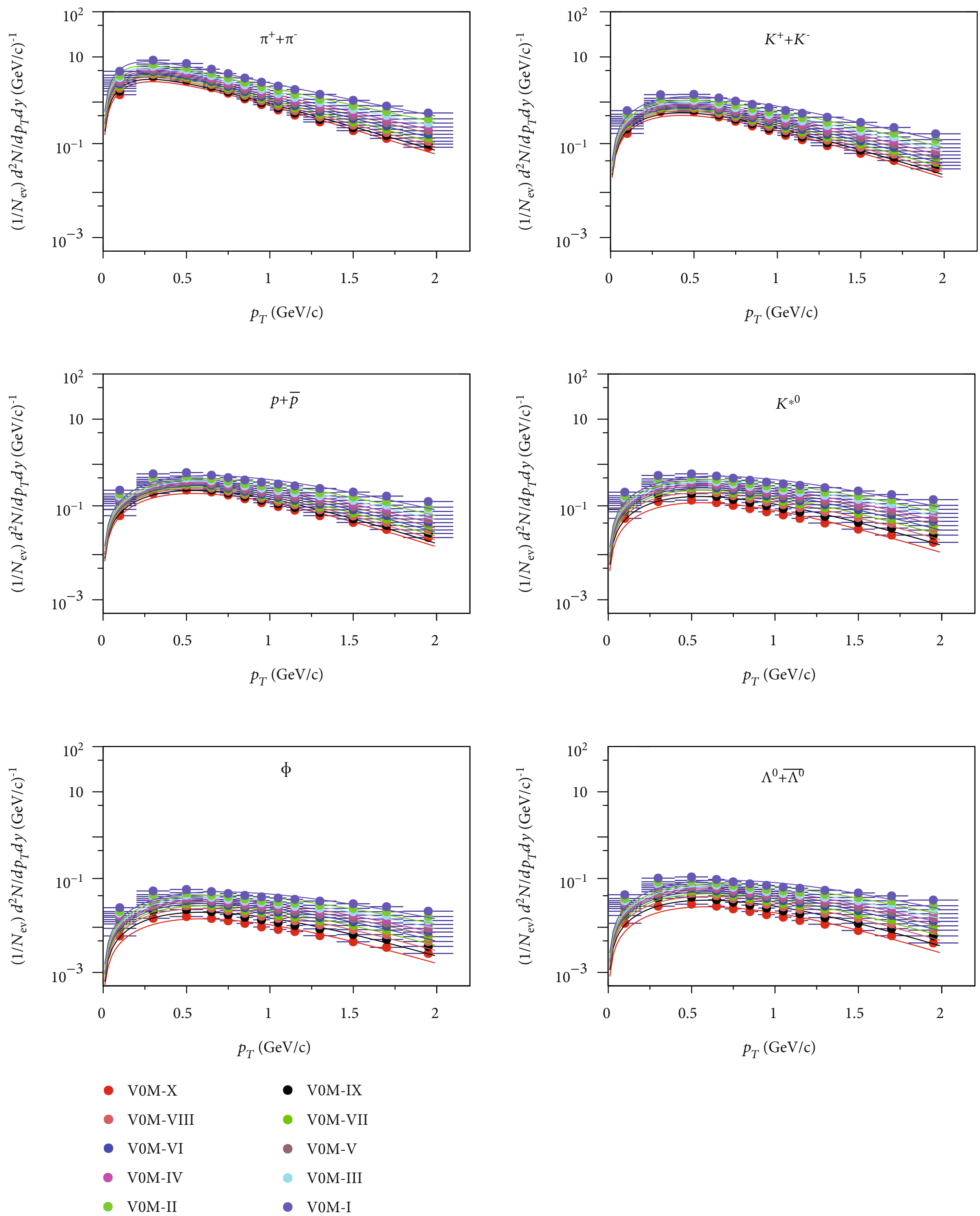

Figure 11: (Color online) Fitting of generated p_T-spectra of identified hadrons from PYTHIA8 using BGBW model for spherocity integrated events in various multiplicity classes as shown in Table 1.

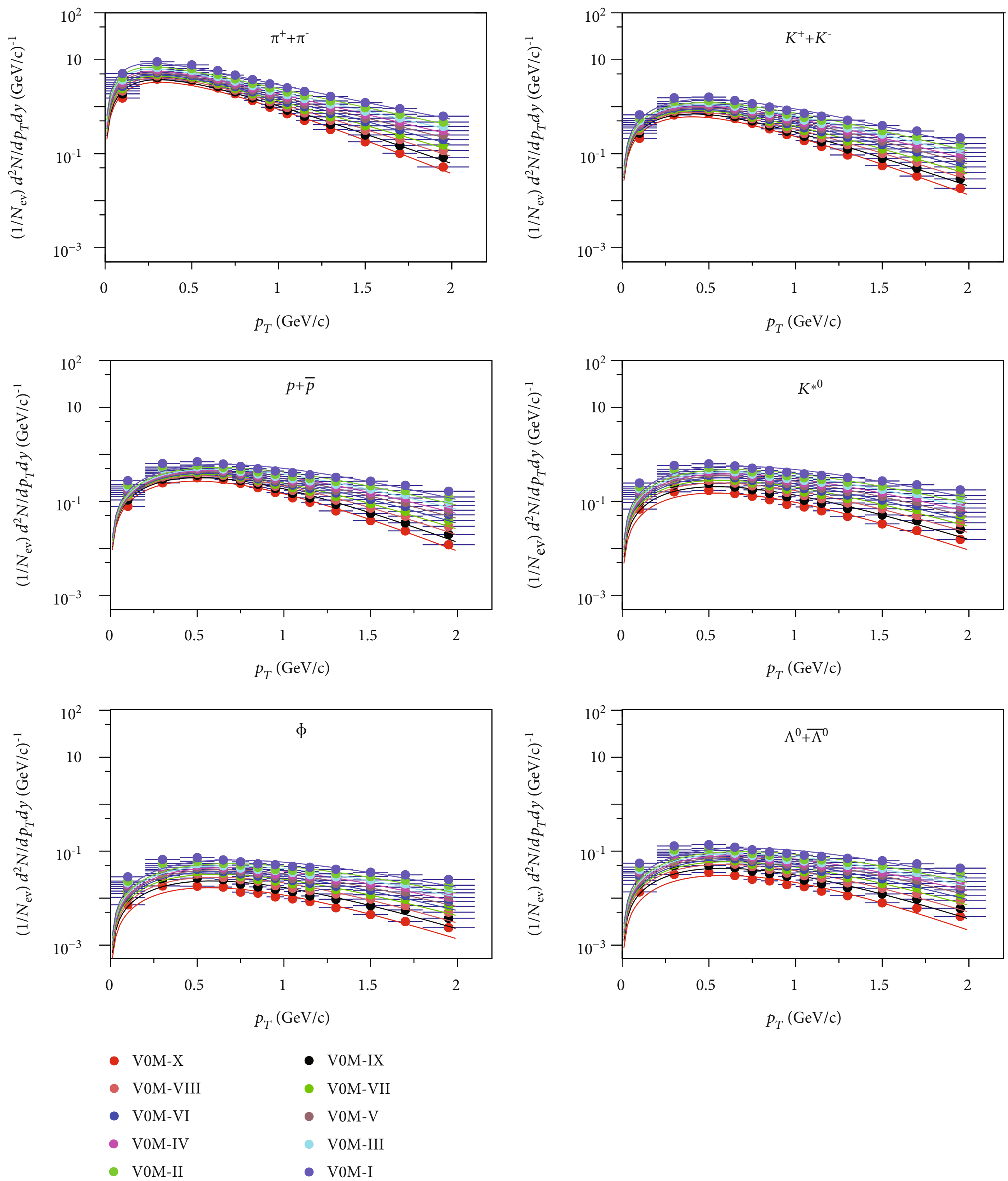

FIGURE 12: (Color online) Fitting of generated p_T-spectra of identified hadrons from PYTHIA8 using the BGBW model for isotropic events in various multiplicity classes as shown in Table 1.

for isotropic events, the nonextensive parameter, q values remain lower compared to the spherocity-integrated events, which suggests that isotropic events have got a higher degree of equilibration compared to spherocity-integrated events. This indicates that while studying the QGP-like conditions in small systems, one should separate the isotropic

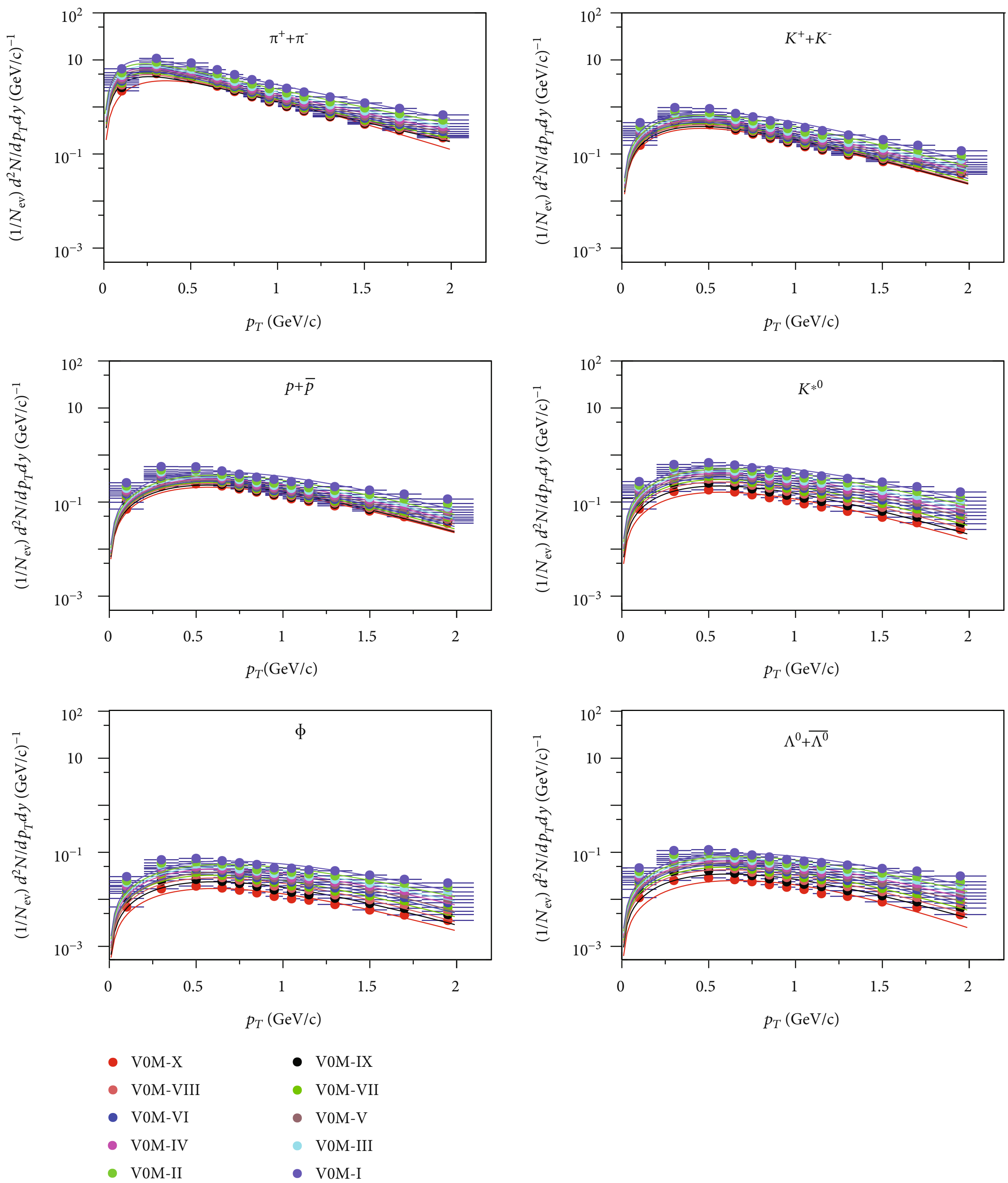

FIGURE 13: (Color online) Fitting of generated p_T-spectra of identified hadrons from PYTHIA8 using the BGBW model for jetty events in various multiplicity classes as shown in Table 1.

events from the spherocity-integrated events, as the production dynamics are different. On the contrary, the q-values for jetty are always higher compared to spherocity-integrated events, indicating that the jetty events remain far away from equilibrium. The present study is very useful in understanding the microscopic features of degrees of

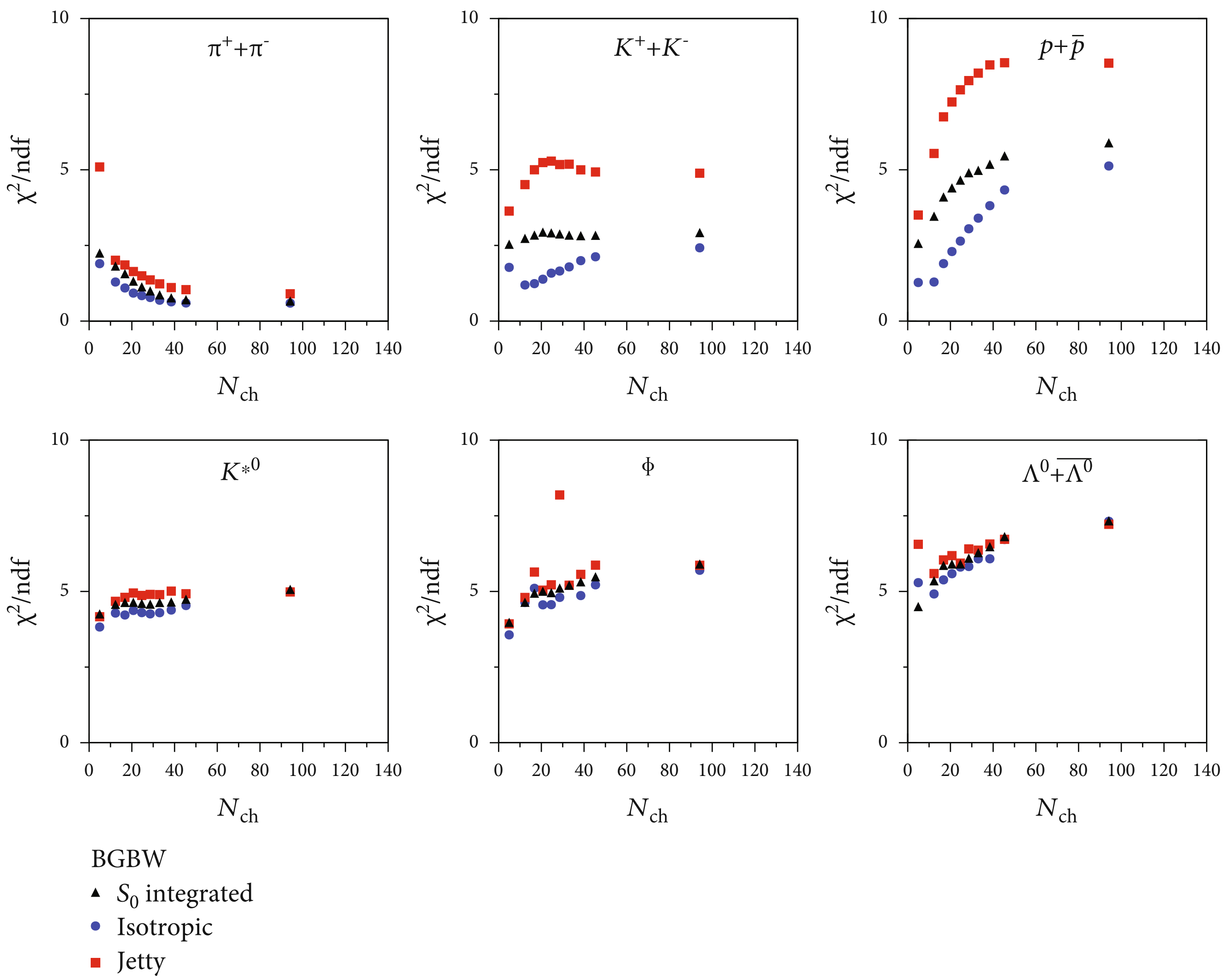

Figure 14: (Color online) χ^2/NDF for the fitting of generated p_T-spectra of identified hadrons using the BGBW model in different spherocity and multiplicity classes.

equilibration and their dependencies on the number of particles in the system and on the geometrical shape of an event. It would be interesting to study the particle mass dependence of these thermodynamic parameters. In order to do that, we have taken the events with the highest multiplicity class and done the same spherocity analysis, taking different particles as discussed here, which is shown in Figure 10. For the isotropic and spherocity-integrated events in high multiplicity pp collisions, the temperature remains higher for particles with higher masses, which supports a differential freeze-out scenario. This suggests that massive particles freeze-out early from the system. However, the jetty events show a reverse trend.

To explore the flow-like features in small systems, one needs to focus on the low-p_T of the particle spectra with Boltzmann-Gibbs Blast-Wave (BGBW) model, which is discussed in the next subsection. As we saw an indication of a differential freeze-out scenario, in the following section, we consider making individual spectral analysis using BGBW, instead of a simultaneous fitting, which is usually necessitated by a single freeze-out scenario.

3.2. Boltzmann-Gibbs Blast-Wave Model. The expression for invariant yield in Boltzmann-Gibbs Blast-Wave (BGBW) model is given by [21, 22]

$$E\frac{d^3N}{dp^3} = D\int d^3\sigma_\mu p^\mu \exp\left(-\frac{p^\mu u_\mu}{T}\right). \quad (5)$$

Here, the four-velocity denoting flow velocities in space-time is given by $u^\mu = \cosh\rho(\cosh\eta, \tanh\rho\cos\phi_r, \tanh\rho\sin\phi_r, \sinh\eta)$, and the particle four-momentum is $p^\mu = (m_T\cosh y, p_T\cos\phi, p_T\sin\phi, m_T\sinh y)$, while the kinetic freeze-out surface is given by $d^3\sigma_\mu = (\cosh\eta, 0, 0, -$

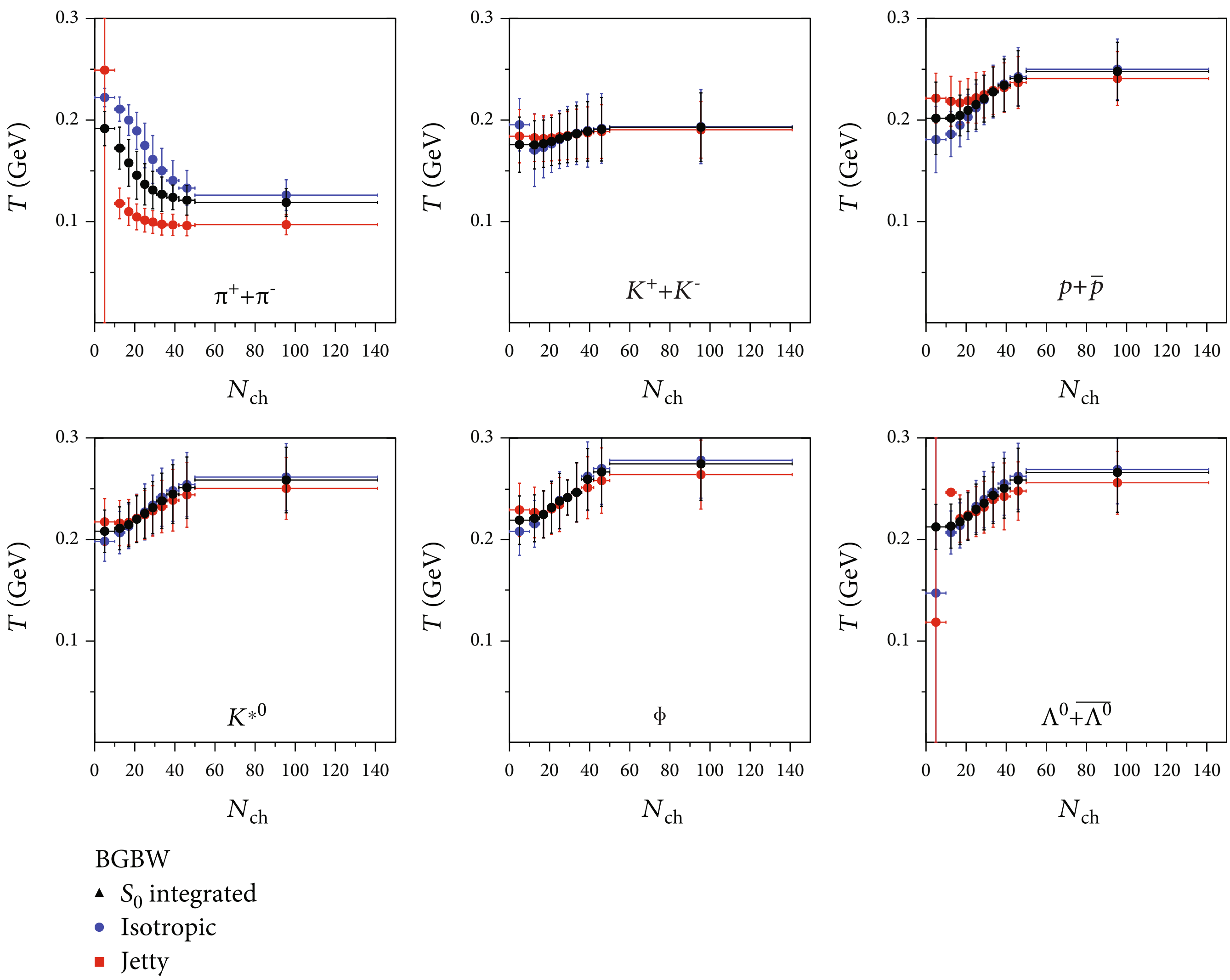

FIGURE 15: (Color online) Multiplicity dependence of T in different spherocity classes from the fitting of the BGBW model.

$\sinh\eta)\tau r dr d\eta d\phi_r$. Here, η is the space-time rapidity and assuming Bjorken correlation in rapidity, i.e., $y=\eta$ [59], Eq. (5) can be expressed as

$$\left.\frac{d^2N}{dp_T dy}\right|_{y=0} = D\int_0^{R_0} r\,dr\,K_1\left(\frac{m_T\cosh\rho}{T}\right)I_0\left(\frac{p_T\sinh\rho}{T}\right). \quad (6)$$

Here, $D = gVm_T/2\pi^2$, where g is the degeneracy factor, V is the system volume, and $m_T=\sqrt{p_T^2+m^2}$ is the transverse mass. Here, $I_0(p_T\sinh\rho/T)$ and $K_1(m_T\cosh\rho/T)$ are the modified Bessel's functions. They are given by

$$K_1\left(\frac{m_T\cosh\rho}{T}\right) = \int_0^\infty \cosh y\,\exp\left(-\frac{m_T\cosh y\cosh\rho}{T}\right)dy, \quad (7)$$

$$I_0\left(\frac{p_T\sinh\rho}{T}\right) = \frac{1}{2\pi}\int_0^{2\pi}\exp\left(\frac{p_T\sinh\rho\cos\phi}{T}\right)d\phi. \quad (8)$$

Here, ρ is a parameter given by $\rho=\tanh^{-1}\beta$. $\beta=\beta_{max}(\xi)^n$ [22, 60–62] is the radial flow, where β_{max} is the maximum surface velocity and $\xi=(r/R_0)$ with r as the radial distance. In the BGBW model, the particles closer to the center of the fireball move slower than the ones at the edges and the average of the transverse velocity can be evaluated as [63]

$$\langle\beta\rangle = \frac{\int\beta_{max}\xi^n\xi\,d\xi}{\int\xi\,d\xi} = \left(\frac{2}{2+n}\right)\beta_{max}. \quad (9)$$

In our calculation, for the sake of simplicity, we use a linear velocity profile, i.e., $n=1$, and R_0 is the

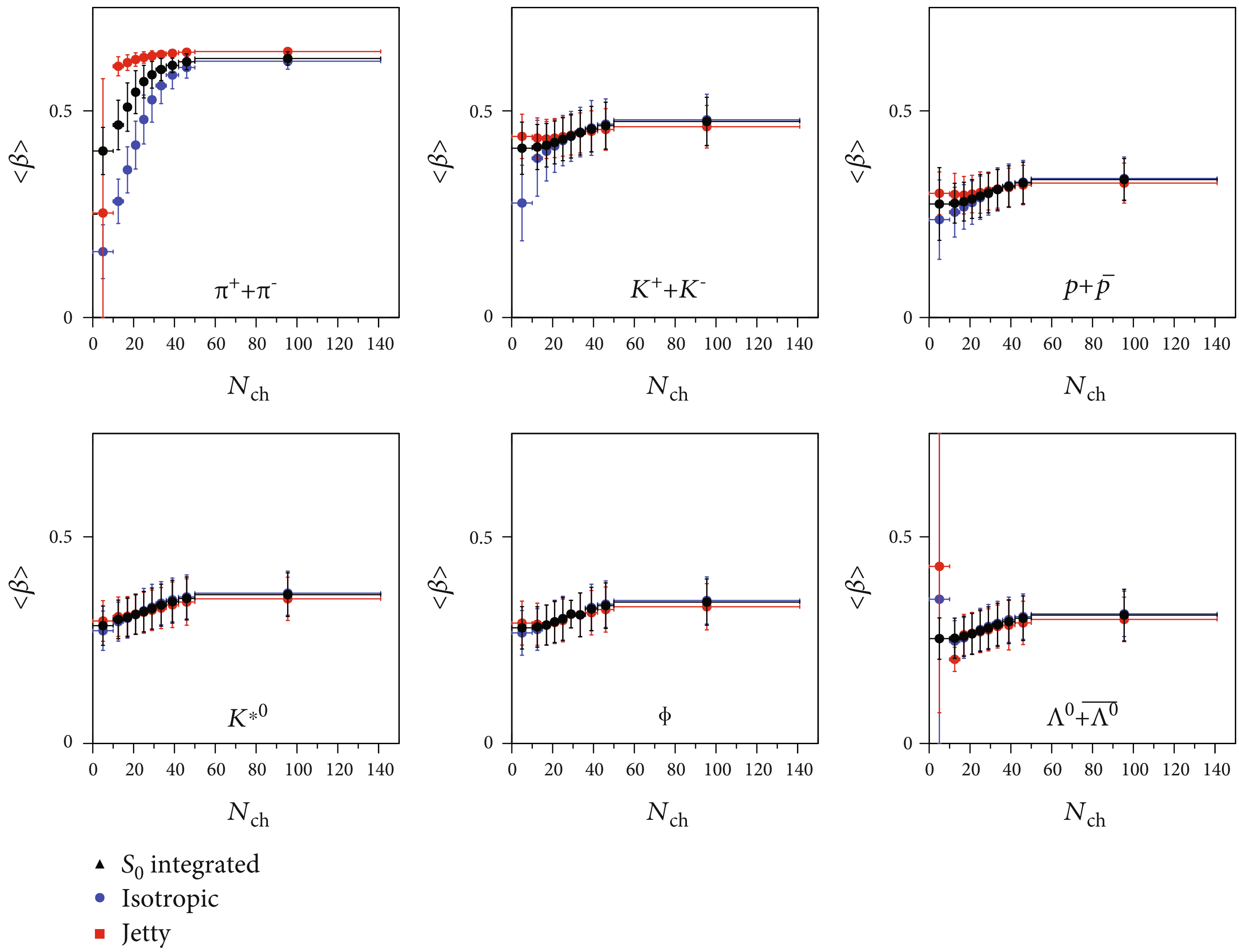

Figure 16: (Color online) Multiplicity dependence of $\langle\beta\rangle$ in different spherocity classes from the fitting of the BGBW model.

maximum radius of the expanding source at freeze-out ($0 < \xi < 1$).

Figures 11–13 show the fitting of p_T-spectra of pions, kaons, protons, K^{*0}, ϕ, and Λ as a function of charged-particle multiplicity using BGBW distribution using Eq. (6) for spherocity-integrated, isotropic, and jetty events, respectively. The BGBW distribution fits the spectra for identified hadrons till $p_T \simeq 2$ GeV/c. Figure 14 shows the χ^2/NDF for the fitting of generated p_T-spectra of identified hadrons using BGBW model in different spherocity and multiplicity classes. For pions, the χ^2/NDF is relatively lower compared to kaons and protons, indicating pions are better described by the BGBW model. The decrease of χ^2/NDF for pions with increasing charged-particle multiplicity is due to the fact that the number of particles is less in the lower multiplicity classes, which makes the fitting worse. As expected, the fitting for jetty events is worse compared to isotropic and spherocity-integrated events, indicating that the jetty events remain far from equilibrium and a BGBW description, hence, becomes less significant.

It is interesting to note that since BGBW analysis is in the soft sector of particle production, as expected, we do not see any difference between jetty, isotropic, and spherocity-integrated events so far the multiplicity dependence of kinetic freeze-out temperature and the radial flow velocity are concerned, except pions. This is depicted in Figures 15 and 16. For all the discussed particles except the pions, the kinetic freeze-out temperature shows a linear increase with final state multiplicity. The radial flow velocity also shows a monotonic increase with multiplicity class for all the particles. Taking the highest multiplicity class, let us now look into the particle mass dependence of the freeze-out parameters. Figure 17 shows that the temperature increases with mass for the highest multiplicity pp collisions, indicating a differential freeze-out scenario. As seen in the previous subsection, the temperature from the BGBW model also suggests that the particles with heavier mass freeze-out early in time. The radial flow velocity is seen to decrease with particle mass, which supports a hydrodynamical behavior. We observe $\langle\beta\rangle \simeq 0.62$ for pions, whereas it is 0.31 for Λ.

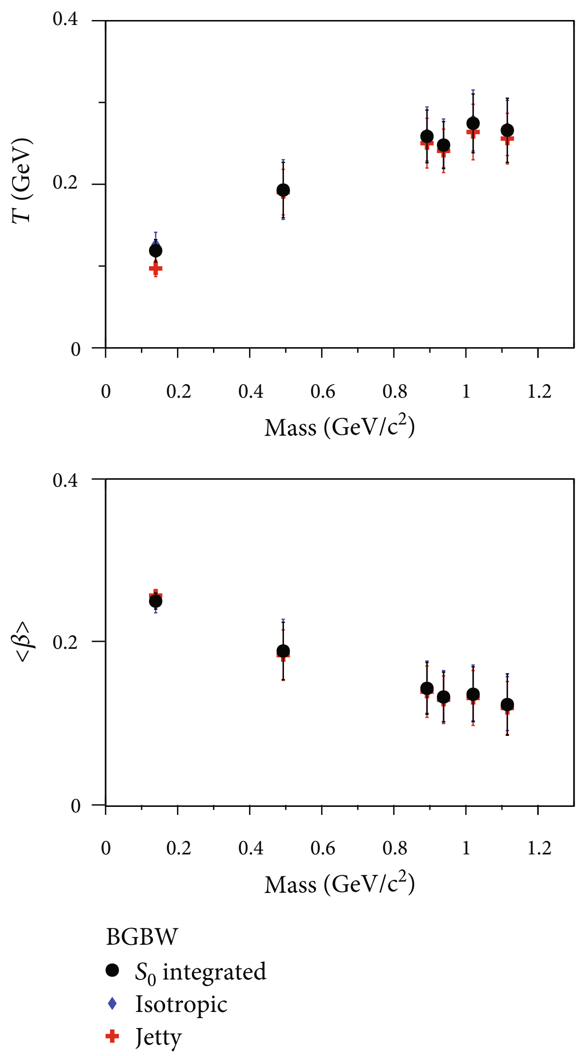

Figure 17: (Color online) Mass dependence of T and $\langle\beta\rangle$ in different spherocity classes for the highest multiplicity class using BGBW fit up to $p_T \sim 2$ GeV/c.

4. Summary and Conclusion

We perform a double differential study of the identified particle spectra and the system thermodynamics as a function of charged-particle multiplicity and transverse spherocity in pp collisions at $\sqrt{s} = 13$ TeV using PYTHIA8. In order to understand the production dynamics of particles in high-multiplicity pp collisions, an event shape-dependent study becomes inevitable. Furthermore, to study the event topology dependence of the kinetic freeze-out properties, we have taken a cosmological expansion scenario of the produced fireball with a differential particle freeze-out. This work would shed light into the underlying event dynamics and help in understanding the possible differences and/or similarities in freeze-out parameters, when the hadronic collisions are compared with heavy-ion collisions. For the analysis of the identified particle p_T-spectra as a function of charged-particle multiplicity and transverse spherocity, we use the thermodynamically consistent and experimentally motivated Tsallis nonextensive distribution function. In the soft sector of particle production, which corresponds to low-p_T, Boltzmann-Gibbs Blast-Wave (BGBW) model is used to extract the kinetic freeze-out temperature and the radial flow velocity to study the particle mass and event multiplicity dependence. The important findings of this work are summarized below:

(i) We observe that the temperature parameter obtained by fitting the full range of the p_T-spectra using Tsallis distribution function is dependent on spherocity class, and it increases with multiplicity for isotropic events, showing a steeper increase for higher mass particles

(ii) The entropic parameter q is found to be spherocity and multiplicity dependent. The jetty events have a tendency of staying away from equilibrium. For isotropic events, the q values remain lower compared to the spherocity-integrated events, which suggests that isotropic events approach more towards equilibrium compared to spherocity-integrated events. This hints for separating isotropic events from spherocity-integrated ones while studying the QGP-like conditions in small systems. This is because the production dynamics are different. In addition, while taking pp collisions as the baseline measurement to study any possible system formation in heavy-ion collisions at the LHC energies, the technique of transverse spherocity would be very useful

(iii) From BGBW analysis, it is observed that the higher mass particles show higher freeze-out temperature, which is an indication of a differential freeze-out scenario

(iv) The radial flow velocity is found to be mass dependent: higher for lighter mass particles—an indication of a hydrodynamic behavior in small systems. The obtained average flow velocities indicate a substantial collectivity in small systems in high multiplicity pp events at the LHC energies

(v) The kinetic freeze-out temperature and the radial flow velocity obtained in the BGBW framework are observed to be independent of spherocity class, except for pions

The present study is very useful in understanding the microscopic features of degrees of equilibration and their dependencies on the number of particles in the system and on the geometrical shape of an event. In the absence of spherocity-dependent experimental data, the present study should give an outlook on similarities/differences between jetty and isotropic events in LHC pp events and their multiplicity dependence. This will help in making a proper bridge in understanding the particle production from hadronic to heavy-ion collisions.

Data Availability

The paper is based on an event generator baseline study paving a way to do similar analysis in experimental data. Data will not be deposited.

Conflicts of Interest

The authors declare that they have no conflicts of interest.

Acknowledgments

The authors acknowledge the financial supports from ALICE Project No. SR/MF/PS-01/2014-IITI(G) of Department of Science & Technology, Government of India. ST acknowledges the financial support by DST-INSPIRE program of the Government of India. RS acknowledges the financial supports from DAE-BRNS Project No. 58/14/29/2019-BRNS of Government of India. Fruitful discussions with Suman Deb and Rutuparna Rath are highly appreciated. The authors would like to acknowledge the usage of resources of the LHC grid computing facility at VECC, Kolkata.

References

[1] J. C. Collins and M. J. Perry, "Superdense matter: neutrons or asymptotically free quarks?," *Physical Review Letters*, vol. 34, no. 21, pp. 1353–1356, 1975.

[2] N. Cabibbo and G. Parisi, "Exponential hadronic spectrum and quark liberation," *Physics Letters B*, vol. 59, no. 1, pp. 67–69, 1975.

[3] ALICE Collaboration, "Enhanced production of multi-strange hadrons in high-multiplicity proton–proton collisions," *Nature Physics*, vol. 13, pp. 535–539, 2017.

[4] S. Tripathy and ALICE Collaboration, "Energy dependence of ϕ (1020) production at mid-rapidity in pp collisions with ALICE at the LHC," *Nuclear Physics A*, vol. 982, pp. 180–182, 2019.

[5] A. K. Dash and ALICE Collaboration, "Multiplicity dependence of strangeness and hadronic resonance production in pp and p-Pb collisions with ALICE at the LHC," *Nuclear Physics A*, vol. 982, pp. 467–470, 2019.

[6] A. Khuntia, H. Sharma, S. Kumar Tiwari, R. Sahoo, and J. Cleymans, "Radial flow and differential freeze-out in proton-proton collisions at $\sqrt{s} = 7$ TeV at the LHC," *European Physical Journal A: Hadrons and Nuclei*, vol. 55, no. 1, p. 3, 2019.

[7] A. Khuntia, S. Tripathy, A. Bisht, and R. Sahoo, "Event shape engineering and multiplicity dependent study of identified particle production in proton+proton pollisions at $\sqrt{s}$= 13 TeV using PYTHIA8," *Journal of Physics G: Nuclear and Particle Physics*, vol. 48, article 035102, 2021.

[8] A. Ortiz Velasquez, P. Christiansen, E. Cuautle Flores, I. Maldonado Cervantes, and G. Paic, "Color reconnection and flowlike patterns in *pp* collisions," *Physical Review Letters*, vol. 111, no. 4, article 042001, 2013.

[9] A. Khatun, D. Thakur, S. Deb, and R. Sahoo, "J/ψ production dynamics: event shape, multiplicity and rapidity dependence in proton+proton collisions at LHC energies using PYTHIA8," *Journal of Physics G: Nuclear and Particle Physics*, vol. 47, no. 5, article 055110, 2020.

[10] T. Sjöstrand, S. Mrenna, and P. Z. Skands, "PYTHIA 6.4 physics and manual," *Journal of High Energy Physics*, vol. 605, p. 26, 2006.

[11] P. Skands, S. Carrazza, and J. Rojo, "Tuning PYTHIA 8.1: the Monash 2013 tune," *European Physical Journal C: Particles and Fields*, vol. 74, no. 8, p. 3024, 2014.

[12] Pythia8, http://home.thep.lu.se/Pythia/.

[13] ALICE Collaboration, "Performance of the ALICE experiment at the CERN LHC," *International Journal of Modern Physics A*, vol. 29, article 1430044, 2014.

[14] E. Cuautle, R. Jimenez, I. Maldonado, A. Ortiz, G. Paic, and E. Perez, "Disentangling the soft and hard components of the pp collisions using the sphero(i)city approach," http://arxiv.org/abs/1404.2372.

[15] A. Ortiz, G. Paic, and E. Cuautle, "Mid-rapidity charged hadron transverse spherocity in pp collisions simulated with Pythia," *Nuclear Physics A*, vol. 941, pp. 78–86, 2015.

[16] A. Ortiz, "Experimental results on event shapes at hadron colliders," *Advanced Series on Directions in High Energy Physics*, vol. 29, p. 343, 2018.

[17] G. P. Salam, "Towards jetography," *European Physical Journal C: Particles and Fields*, vol. 67, no. 3-4, pp. 637–686, 2010.

[18] G. Bencédi and ALICE Collaboration, "Event-shape-and multiplicity-dependent identified particle production in pp collisions at 13 TeV with ALICE at the LHC," *Nuclear Physics A*, vol. 982, pp. 507–510, 2019.

[19] ALICE Collaboration, "Pseudorapidity and transverse-momentum distributions of charged particles in proton–proton collisions at $\sqrt{s}$=13 TeV," *Physics Letters B*, vol. 753, pp. 319–329, 2016.

[20] J. Cleymans and D. Worku, "The Tsallis distribution in proton–proton collisions at $\sqrt{s} = 0.9$ TeV at the LHC," *Journal of Physics G: Nuclear and Particle Physics*, vol. 39, no. 2, article 025006, 2012.

[21] F. Cooper and G. Frye, "Single-particle distribution in the hydrodynamic and statistical thermodynamic models of multiparticle production," *Physical Review D*, vol. 10, no. 1, pp. 186–189, 1974.

[22] E. Schnedermann, J. Sollfrank, and U. W. Heinz, "Thermal phenomenology of hadrons from 200AGeV S+S collisions," *Physical Review C*, vol. 48, no. 5, pp. 2462–2475, 1993.

[23] R. Hagedorn, "Statistical thermodynamics of strong interactions at high energies," *II Nuovo Cimento*, vol. 3, pp. 147–186, 1965.

[24] C. Michael and L. Vanryckeghem, "Consequences of momentum conservation for particle production at large transverse momentum," *Journal of Physics G: Nuclear Physics*, vol. 3, no. 8, pp. L151–L156, 1977.

[25] C. Michael, "Large transverse momentum and large mass production in hadronic interactions," *Progress in Particle and Nuclear Physics*, vol. 2, pp. 1–39, 1979.

[26] UA1 Collaboration, "Transverse momentum spectra for charged particles at the CERN proton-antiproton collider," *Physics Letters B*, vol. 118, no. 1-3, p. 167, 1982.

[27] R. Hagedorn, "Multiplicities, p_T distributions and the expected hadron→quark-gluon phase transition," *La Rivista del Nuovo Cimento*, vol. 6, no. 10, p. 1, 1983.

[28] STAR Collaboration, "Strange particle production in $p + p$ collisions at $\sqrt{s} = 200$ GeV," *Physical Review C*, vol. 75, article 064901, 2007.

[29] PHENIX Collaboration, "Identified charged hadron production in $p + p$ collisions at $\sqrt{s}$ = 200 and 62.4 GeV," *Physical Review C*, vol. 83, article 064903, 2011.

[30] ALICE Collaboration, "Production of pions, kaons and protons in pp collisions at $\sqrt{s}$ = 900 GeV with ALICE at the LHC," *The European Physical Journal C*, vol. 71, article 1655, 2011.

[31] ALICE Collaboration, "Neutral pion and η meson production in proton–proton collisions at $\sqrt{s}$ = 0.9 TeV and $\sqrt{s}$ = 7 TeV," *Physics Letters B*, vol. 717, no. 1-3, pp. 162–172, 2012.

[32] ALICE Collaboration, "Multi-strange baryon production in *pp* collisions at $\sqrt{s}$ = 7 TeV with ALICE," *Physics Letters B*, vol. 712, p. 309, 2012.

[33] ALICE Collaboration, "Study of the inclusive production of charged pions, kaons, and protons in pp collisions at $\sqrt{s}$ = 0.9, 2.76, and 7 TeV," *The European Physical Journal C*, vol. 72, article 2164, 2012.

[34] T. Bhattacharyya, P. Garg, R. Sahoo, and P. Samantray, "Time evolution of temperature fluctuation in a non-equilibrated system," *European Physical Journal A: Hadrons and Nuclei*, vol. 52, no. 9, p. 283, 2016.

[35] T. Bhattacharyya, J. Cleymans, A. Khuntia, P. Pareek, and R. Sahoo, "Radial flow in non-extensive thermodynamics and study of particle spectra at LHC in the limit of small (q - 1)," *European Physical Journal A: Hadrons and Nuclei*, vol. 52, no. 2, p. 30, 2016.

[36] H. Zheng and L. Zhu, "Can Tsallis distribution fit all the particle spectra produced at RHIC and LHC?," *Advances in High Energy Physics*, vol. 2015, Article ID 180491, 9 pages, 2015.

[37] Z. Tang, Y. Xu, L. Ruan, G. van Buren, F. Wang, and Z. Xu, "Spectra and radial flow in relativistic heavy ion collisions with Tsallis statistics in a blast-wave description," *Physical Review C*, vol. 79, no. 5, article 051901, 2009.

[38] B. De, "Non-extensive statistics and understanding particle production and kinetic freeze-out process from p_T-spectra at 2.76 TeV," *European Physical Journal A: Hadrons and Nuclei*, vol. 50, no. 9, p. 138, 2014.

[39] I. Bediaga, E. M. F. Curado, and J. M. de Miranda, "A nonextensive thermodynamical equilibrium approach in $e^+e^- \rightarrow$ hadrons," *Physica A*, vol. 286, no. 1-2, pp. 156–163, 2000.

[40] G. Wilk and Z. Włodarczyk, "Quasi-power law ensembles," *Acta Physica Polonica B*, vol. 46, no. 6, article 1103, 2015.

[41] K. Ürmössy, G. G. Barnaföldi, and T. S. Biró, "Generalised Tsallis statistics in electron–positron collisions," *Physics Letters B*, vol. 701, no. 1, pp. 111–116, 2011.

[42] K. Ürmössy, G. G. Barnaföldi, and T. S. Biró, "Microcanonical jet-fragmentation in proton–proton collisions at LHC energy," *Physics Letters B*, vol. 718, no. 1, pp. 125–129, 2012.

[43] P. K. Khandai, P. Sett, P. Shukla, and V. Singh, "Hadron spectra in p+p collisions at RHIC and LHC energies," *International Journal of Modern Physics A*, vol. 28, no. 16, article 1350066, 2013.

[44] B.-C. Li, Y.-Z. Wang, and F.-H. Liu, "Formulation of transverse mass distributions in Au–Au collisions at $\sqrt{s_{NN}}$= 200 GeV/nucleon," *Physics Letters B*, vol. 725, no. 4-5, pp. 352–356, 2013.

[45] L. Marques, J. Cleymans, and A. Deppman, "Description of high-energy *pp* collisions using Tsallis thermodynamics: transverse momentum and rapidity distributions," *Physical Review D*, vol. 91, article 054025, 2015.

[46] PHENIX collaboration, "Measurement of neutral mesons in $p + p$ collisions at $\sqrt{s}$ = 200 GeV and scaling properties of hadron production," *Physical Review D*, vol. 83, article 052004, 2011.

[47] ALICE collaboration, "Transverse momentum spectra of charged particles in proton–proton collisions at $\sqrt{s}$ = 900 GeV with ALICE at the LHC," *Physics Letters B*, vol. 693, no. 2, pp. 53–68, 2010.

[48] ALICE collaboration, "Production of pions, kaons and protons in pp collisions at $\sqrt{s}$=200 GeV with ALICE at the LHC," *The European Physical Journal C*, vol. 71, article 1655, 2011.

[49] CMS collaboration, "Transverse-momentum and pseudorapidity distributions of charged hadrons in pp collisions at $\sqrt{s}$ = 0.9 and 2.36 TeV," *Journal of High Energy Physics*, vol. 2, p. 41, 2010.

[50] CMS collaboration, "Transverse-momentum and pseudorapidity distributions of charged hadrons in *pp* collisions at $\sqrt{s}$=7 TeV," *Physical Review Letters*, vol. 105, article 022002, 2010.

[51] ATLAS collaboration, "Charged-particle multiplicities in pp interactions measured with the ATLAS detector at the LHC," *New Journal of Physics*, vol. 13, article 053033, 2011.

[52] ALICE collaboration, "Pion, kaon, and proton production in central Pb-Pb collisions at $\sqrt{s_{NN}}$ = 2.76 TeV," *Physical Review Letters*, vol. 109, article 252301, 2012.

[53] S. Grigoryan, "Using the Tsallis distribution for hadron spectra inppcollisions: pions and quarkonia at $\sqrt{s}$ = 5−13000 GeV," *Physical Review D*, vol. 95, no. 5, article 056021, 2017.

[54] A. S. Parvan, O. V. Teryaev, and J. Cleymans, "Systematic comparison of Tsallis statistics for charged pions produced in pp collisions," *European Physical Journal A: Hadrons and Nuclei*, vol. 53, no. 5, p. 102, 2017.

[55] J. Cleymans, G. I. Lykasov, A. S. Parvan, A. S. Sorin, O. V. Teryaev, and D. Worku, "Systematic properties of the Tsallis distribution: energy dependence of parameters in high energy p-p collisions," *Physics Letters B*, vol. 723, no. 4-5, pp. 351–354, 2013.

[56] C. Tsallis, *Introduction to Nonextensive Statistical Mechanics*, Springer, 2009.

[57] C. Beck, "Superstatistics: theory and applications," *Continuum Mechanics and Thermodynamics*, vol. 16, no. 3, pp. 293–304, 2004.

[58] G. Wilk and Z. Wlodarczyk, "Interpretation of the nonextensivity parameterqin some applications of Tsallis statistics and Lévy distributions," *Physical Review Letters*, vol. 84, no. 13, pp. 2770–2773, 2000.

[59] J. D. Bjorken, "Highly relativistic nucleus-nucleus collisions: the central rapidity region," *Physical Review D*, vol. 27, no. 1, pp. 140–151, 1983.

[60] P. Huovinen, P. F. Kolb, U. W. Heinz, P. V. Ruuskanen, and S. A. Voloshin, "Radial and elliptic flow at RHIC: further predictions," *Physics Letters B*, vol. 503, no. 1-2, pp. 58–64, 2001.

[61] P. Braun-Munzinger, J. Stachel, J. P. Wessels, and N. Xu, "Thermal equilibration and expansion in nucleus-nucleus collisions at the AGS," *Physics Letters B*, vol. 344, p. 43, 1995.

[62] Z.-B. Tang, L. Yi, L.-J. Ruan et al., "The statistical origin of constituent-quark scaling in QGP hadronization," *Chinese Physics Letters*, vol. 30, no. 3, article 031201, 2013.

[63] PHENIX Collaboration, "Single identified hadron spectra from $\sqrt{s_{NN}}$=130GeV Au+Au collisions," *Physical Review C*, vol. 69, article 024904, 2004.